

# Mechanistic and Thermodynamic Evaluation of Molnupiravir Binding to Bovine Serum Albumin Using Fluorescence Spectroscopy and *In Silico* Analysis

Mohiminul Adib<sup>1</sup>, Osama Bin Abul Hossain<sup>1,2</sup>, Suparna Dutta Pinki<sup>1</sup>,  
Md Abdus Samadd<sup>1,2</sup> and Md. Zakir Sultan<sup>3</sup>

<sup>1</sup>Department of Pharmaceutical Chemistry, Faculty of Pharmacy, University of Dhaka, Dhaka-1000, Bangladesh

<sup>2</sup>Department of Pharmacy, Faculty of Science and Engineering, International Islamic University Chittagong, Kumira-4318, Bangladesh

<sup>3</sup>Centre for Advanced Research in Sciences, University of Dhaka, Dhaka-1000, Bangladesh

(Received: March 15, 2026; Accepted: June 10, 2026; Published (web): June 25, 2026)

**ABSTRACT:** Protein binding regulates a drug's pharmacokinetics, bioavailability and therapeutic efficacy. This study explores the interaction between the antiviral drug Molnupiravir and bovine serum albumin (BSA), 76% of whose sequence is homologous to human serum albumin and widely accepted in preliminary drug-protein interaction studies, to determine binding mechanisms and pharmacokinetic effects. Fluorescence spectroscopy at physiological pH (7.4) and temperatures (302 and 310 K, representing normal and febrile physiological conditions, respectively) showed concentration-dependent quenching at excitation wavelengths of 280 and 293 nm, indicating the involvement of tryptophan and tyrosine residues in the binding interaction. The Stern-Volmer analysis affirmed a dynamic quenching operation, with constants increasing from 0.0166 to 0.0176  $\mu\text{M}^{-1}$ . Thermodynamic parameters indicate spontaneous, entropy-driven binding ( $\Delta G = -24.4$  kJ/mol at 302 K), dominated by hydrophobic interactions. Using AutoDock Vina, binding at Sudlow site I was discovered with an affinity of -7.9 kcal/mol, involving critical residues GLY327 and ARG208.

**Key words:** Molnupiravir; Bovine Serum Albumin; Fluorescence Spectroscopy; Drug-Protein Interaction; Thermodynamics

## INTRODUCTION

The binding of a drug to plasma proteins affects its therapeutic potential, bioavailability, and efficacy. Drugs mainly interact with serum albumin, which makes up about 60% of plasma proteins.<sup>1</sup> These interactions impact free drug levels, as only unbound drugs can pass cell membranes to reach targets. Therefore, understanding binding is essential for predicting drug behavior and adjusting doses.<sup>2</sup>

Bovine Serum Albumin (BSA) is often used as a protein model for drug-protein binding because 76% of its sequence is homologous to human serum albumin (HSA).<sup>3</sup> BSA (MW 66,210 Da) is a globular

protein with 585 amino acids in three domains, 17 disulfide bonds, a free cysteine at residue 34 and two tryptophans at residues 134 and 212.<sup>4</sup>

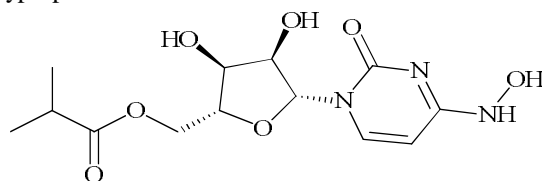


Figure 1. Molecular Structure of Molnupiravir.

Molnupiravir (MK-4482/EIDD-2801, Figure 1) is an approved oral antiviral for emergency use with mild to moderate COVID-19, a global outbreak cause of millions of deaths.<sup>5,6</sup> As a prodrug of N4-Hydroxycytidine (NHC), it is rapidly metabolized into NHC-triphosphate (NHC-TP).

**Correspondence to:** Md. Abdus Samadd  
Email: samadd@iiuc.ac.bd

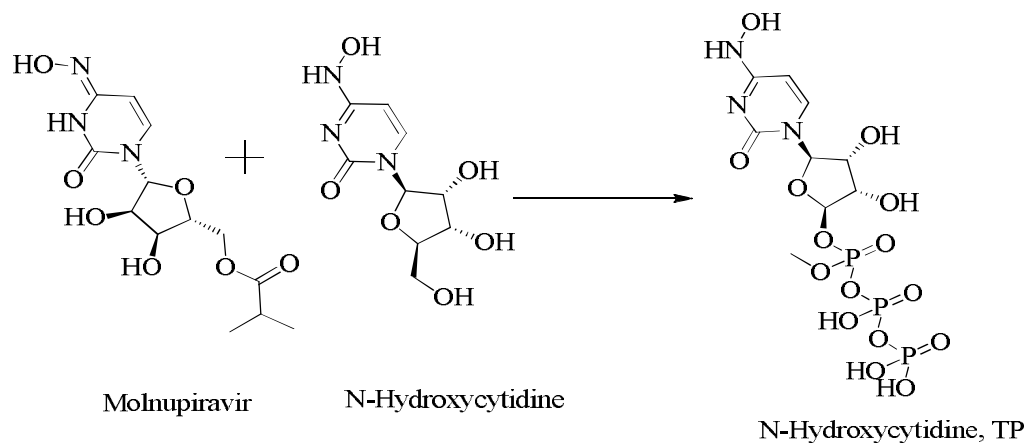


Figure 2. Metabolic activation pathway of molnupiravir to NHC-triphosphate

This compound acts as a ribonucleoside analog incorporated into viral RNA during replication.<sup>7</sup> When integrated, NHC-TP exhibits ambiguous base pairing, sometimes mimicking cytidine and other times uridine, leading to mutations (C—U and G—A). Over multiple cycles, these mutations accumulate beyond the virus's repair ability, causing lethal mutagenesis or viral error catastrophe, thereby halting replication.<sup>8</sup>

Although molnupiravir is rapidly hydrolyzed to its primary circulating metabolite, NHC, before systemic entry, understanding the albumin-binding properties of the parent prodrug remains important for characterizing early distribution.<sup>9,10</sup>

Despite its clinical importance, comprehensive data on Molnupiravir's protein-binding properties remain limited. Regulatory assessments have shown that plasma protein binding of Molnupiravir cannot be precisely measured due to its instability in plasma. In contrast, its active metabolite, NHC, exhibits an unbound fraction of about 1, indicating minimal protein binding across various matrices and concentrations.<sup>10,11</sup> However, the mechanistic binding parameters of the parent compound—such as binding constants, stoichiometry, thermodynamic profiles, and molecular interactions—are still uncharacterized, leaving a gap in pharmacokinetic knowledge. This study employs fluorescence spectroscopy to

investigate molnupiravir's interaction with BSA under physiological conditions. The aims are to: (1) elucidate the mechanism of BSA fluorescence quenching by molnupiravir; (2) determine binding constants and stoichiometry at relevant temperatures; (3) analyze thermodynamic parameters ( $\Delta G$ ,  $\Delta H$ ,  $\Delta S$ ) and (4) identify the molecular forces involved. These findings are crucial for understanding pharmacokinetics, predicting drug interactions, and guiding dosing strategies.

## MATERIALS AND METHODS

**Materials.** Molnupiravir ( $C_{13}H_{19}N_3O_7$ , 329.31 g/mol, 99.99% purity) was procured from MedChemExpress (MCE), USA, as a white crystalline powder. It exhibited a maximum absorption wavelength ( $\lambda_{max}$ ) at 235 nm. Bovine Serum Albumin (fraction V, 96–99% purity, fatty acid-free, molecular weight 66210 Da) was supplied by Sigma Chemical Co., USA. Analytical-grade disodium hydrogen phosphate ( $Na_2HPO_4$ ; 141.96 g/mol) and potassium dihydrogen phosphate ( $KH_2PO_4$ ; 136.09 g/mol) were acquired from Glaxo, United Kingdom. Analytical-grade methanol, ethanol and deionized water were employed as solvents throughout the study. A fluorescence spectrophotometer (Hitachi FL-7000, Japan) and a spectrophotometer (UV-1800, Shimadzu) were

utilized for recording absorption values. Moreover, a metabolic shaking incubator (Fisher Scientific, UK), a water bath (Unitronic Orbital, P-Spectra, Spain), micropipettes (ZONGTAI Biomedical, China), an analytical balance (AND GH-200, UK), a pH meter (Hanna Instrument & Co., USA) and a temperature-controlled oven (Mettler, Germany) were utilized in this research.

### Sample preparation

**Buffer solution.** A buffer (phosphate, pH 7.4) was prepared following the previous method (Perrin, 2012) through  $\text{Na}_2\text{HPO}_4$  solution and  $\text{KH}_2\text{PO}_4$  solution.

**Protein and drug solution.** A stock solution (10  $\mu\text{M}$  of BSA) was prepared in the phosphate buffer solution. A 1 mM molnupiravir stock solution was prepared using deionized water. Both solutions were kept at 4°C until needed. All necessary precautions were taken to prevent foam formation. Since molnupiravir was prepared in deionized water—the same bulk solvent as the phosphate buffer—the final assay solutions contained  $\leq 1\%$  v/v water after mixing, which cannot significantly alter buffer pH or ionic strength due to the phosphate system's buffering capacity.<sup>12</sup>

### Sample preparation for fluorescence titration

**Standard curve preparation.** A standard curve (absorbance vs. concentration) has been prepared to calculate the strength of Molnupiravir in the sample. Varying concentrations of Molnupiravir were generated through serial dilution (10, 20, 40, 60, 80, 120, and 160  $\mu\text{M}$ ). After thorough mixing, absorbance was measured at 235 nm using a UV spectrophotometer, with a buffer solution as the reference. The 235 nm wavelength was chosen because it aligns with molnupiravir's absorption maximum ( $\lambda_{\text{max}}$ ), representing the  $\pi \rightarrow \pi$  electronic transition of its nucleoside analog chromophore, where analytical sensitivity is optimal and minor wavelength shifts minimally affect absorbance.<sup>13,14</sup> Although BSA shows background absorbance below 250 nm, interference was prevented by using a 10  $\mu\text{M}$

BSA solution at pH 7.4 as the reference blank, ensuring that absorbance readings solely reflected molnupiravir.

**Sample preparation and absorbance.** For absorbance measurements of Molnupiravir and BSA, a 10  $\mu\text{M}$  BSA (pH 7.4) solution was considered. A serial dilution was used to generate concentrations of Molnupiravir at 10, 20, 40, 60, 80, 120 and 160  $\mu\text{M}$ . The control group was the BSA solution in buffer. All samples were thoroughly mixed for 2 minutes, then equilibrated at the two experimental temperatures, 302K and 310K, for 25 minutes before fluorescence measurements. This procedure was repeated four times: (1) 302K with 280 nm excitation, (2) 302K with 293 nm excitation, (3) 310K with 280 nm excitation, and (4) 310K with 293 nm excitation. The excitation wavelength of 280 nm was selected because it simultaneously excites both tryptophan (Trp) and tyrosine (Tyr) residues of BSA, whereas 293 nm provides selective excitation of tryptophan residues only; this dual-wavelength approach allows discrimination of the individual contributions of each fluorophore type to the observed quenching and provides deeper mechanistic insight into the residues primarily involved in drug–protein binding.<sup>15,16</sup>

**Fluorescence spectroscopy measurements and quenching analysis.** The mechanism and efficiency of fluorescence quenching (Stern-Volmer equation) were evaluated:

$$\frac{F_0}{F} = 1 + K_{sv} [Q]$$

$F_0$  represents the fluorescence intensity of BSA without Molnupiravir, whereas  $F$  indicates the fluorescence intensity in its presence. The symbol  $[Q]$  signifies the Molnupiravir strength and  $K_{sv}$  denotes quenching constant (Stern-Volmer). Values of  $K_{sv}$  were derived from the linear graph slope by plotting  $F_0/F$  against  $[Q]$ . The temperature dependence of  $K_{sv}$  was utilized to discern between dynamic and static quenching.<sup>15,17,18</sup> All fluorescence measurements were performed in triplicate ( $n = 3$ ) and the data were calculated as mean  $\pm$  standard deviation (SD).

**Thermodynamic parameters.** Two physiologically relevant temperatures (302 K and 310 K), representing near-normal and mild febrile body states, respectively, were employed for thermodynamic analysis. This two-point Van't Hoff approach aligns with common practice in drug-BSA fluorescence quenching, where two-temperature designs are used to obtain reliable thermodynamic parameters.<sup>9,10,16</sup> The equation (Van't Hoff)<sup>19</sup> was used to determine the thermodynamic parameters that were essential for the binding interaction

$$\ln K_{sv} = \frac{-\Delta H}{RT} + \frac{\Delta S}{R}$$

Where  $\Delta H$  and  $\Delta S$  are equal to the change in enthalpy and entropy, respectively.  $R = 8.314 \text{ J mol}^{-1} \text{ K}^{-1}$  (universal gas constant),  $T$  signifies the absolute temperature and  $K_{sv}$  is the binding constant at that temperature. The  $\Delta S$  and  $\Delta H$  values were derived from the intercept and slope of the linear plot ( $\ln K_{sv}$  versus  $1/T$ ).<sup>15,19</sup> The Gibbs free energy ( $\Delta G$ ) was determined using the following equation:

$$\Delta G = \Delta H - T\Delta S$$

**Binding constants and stoichiometry.**  $K$  (binding constant) and the frequency of binding sites per albumin molecule ( $n$ ) were determined by utilizing the double logarithmic equation. The  $K$  and  $n$  values were obtained from the intercept and slope, respectively ( $\log [(F_0-F)/F]$  versus  $\log [Q]$ ).<sup>17,18</sup>

$$\log\left[\frac{F_0 - F}{F}\right] = \log K + n \log [Q]$$

**Molecular docking.** The 3D structure of BSA (PDB ID: 4f5s) was obtained from the RCSB Protein Data Bank in PDB format to study molnupiravir interactions. BSA is a homodimer of two chains, A and B; chain B was used for docking. Discovery Studio 2020 prepared the protein by removing water and co-structures, then performed energy minimization using conjugate gradient and steepest descent methods. Energy calculations were performed in vacuo with GROMOS 96 43B1 in Swiss-PDB Viewer. PDB files were converted to pdbqt using AutoDock Tools. Molnupiravir was obtained from PubChem in SDF, exported to PDB via Open Babel, and then converted to PDBQT. Docking

analysis was performed using AutoDock Vina. The docking search space was centered at  $X = 24.51 \text{ \AA}$ ,  $Y = 31.84 \text{ \AA}$ , and  $Z = 18.27 \text{ \AA}$ , with grid box dimensions of  $30 \text{ \AA} \times 30 \text{ \AA} \times 30 \text{ \AA}$ . Binding affinities were reported in kcal/mol. The process was automated with a provided shell script, with ligand affinities in kcal/mol. Visualization of interactions was done in Discovery Studio 2020.

## RESULTS AND DISCUSSION

### UV-Visible spectroscopy and standard curve.

The UV-visible spectrum of molnupiravir exhibited a characteristic absorption peak at 235 nm, aligning with its nucleoside analog structure. A calibration curve generated over a concentration range of 10–160  $\mu\text{M}$  demonstrated excellent linearity ( $R^2 = 0.9942$ ; Figure 3), confirming compliance with the Beer-Lambert law and allowing precise quantification of molnupiravir in the binding studies.

**Fluorescence quenching studies.** Upon excitation of BSA at 280 nm and 293 nm, characteristic emission maxima at  $\sim 340 \text{ nm}$  were observed. The fluorescence intensity decreased gradually with increasing molnupiravir concentration at both wavelengths, indicating a concentration-dependent binding interaction (Table 1). Quenching at 280 nm (exciting both tryptophan and tyrosine) and 293 nm (selective for tryptophan) suggests the interaction mainly affects tryptophan residues. The higher  $F_0/F$  values at 293 nm compared to 280 nm further support tryptophan's primary involvement. As shown in Table 1,  $F_0/F$  ratios increased with higher molnupiravir concentrations at both temperatures, confirming binding.

**Stern-volmer analysis.** Table 2 shows that the Stern-Volmer quenching constant increased from  $0.0166 \mu\text{M}^{-1}$  at 302K to  $0.0176 \mu\text{M}^{-1}$  at 310K. The linear Stern-Volmer plots and high correlation coefficients suggest that a single quenching mechanism is at work in these experiments. Figure 4 shows that these plots ( $F_0/F$  vs [Molnupiravir]) are highly linear at both temperatures. The quenching constants ( $K_{sv}$ ) were obtained from the slopes.

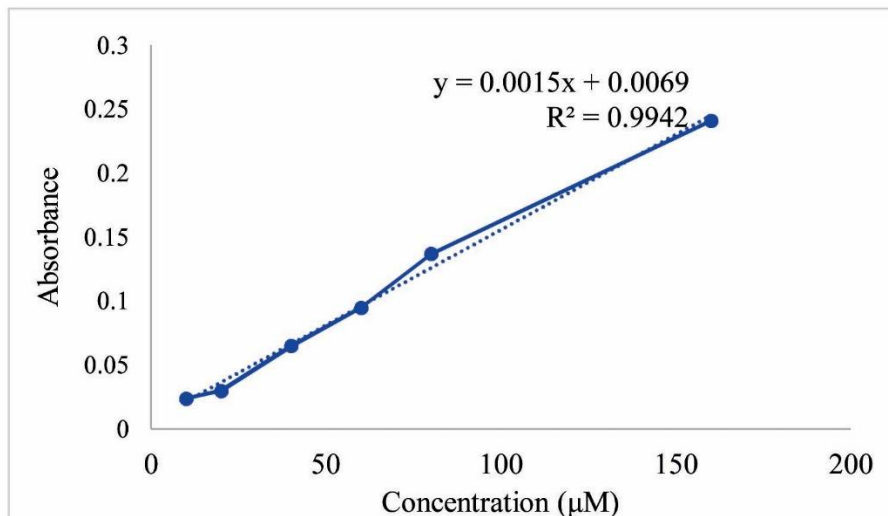
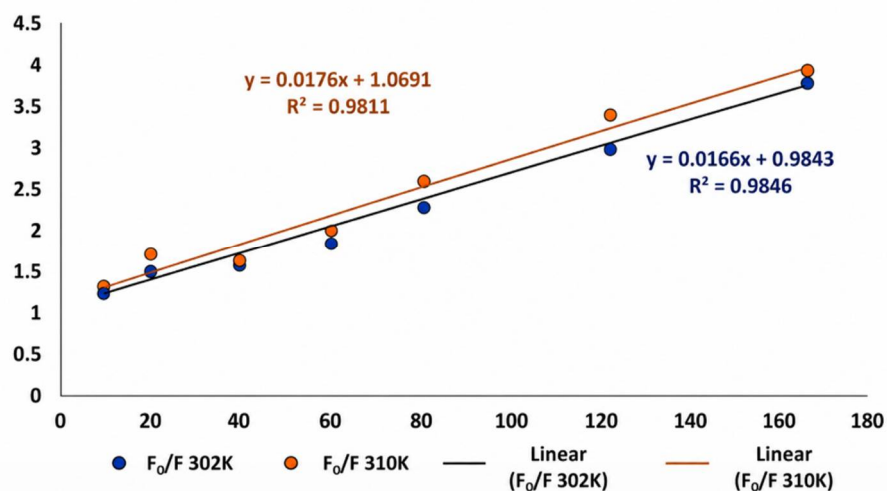


Figure 3. Standard curve of Molnupiravir

Table 1. Fluorescence quenching data at 302K and 310K.

[Molnupiravir]/[BSA]	F <sub>0</sub> /F (302K, 280nm)	F <sub>0</sub> /F (302K, 293nm)	F <sub>0</sub> /F (310K, 280nm)	F <sub>0</sub> /F (310K, 293nm)
1	1.251	1.375	1.264	1.335
2	1.447	1.766	1.598	1.549
4	1.554	1.736	1.604	1.635
6	1.819	2.198	1.966	1.997
8	2.248	2.586	2.522	2.318
12	2.975	3.798	3.314	2.704
16	3.744	4.060	3.846	3.881



\*Molnupiravir concentrations on the x-axis are expressed in µM; Fluorescence intensity ratio is expressed in F<sub>0</sub>/F in y-axis.

Figure 4. Stern-Volmer plots for the BSA-Molnupiravir system at 302K and 310K

**Table 2. Stern-Volmer quenching constants at different temperatures.**

Temperature (K)	$K_{sv}$ ( $\mu\text{M}^{-1}$ )	$R^2$
302	0.0166	0.995
310	0.0176	0.997

**Thermodynamic parameters.** Thermodynamic parameters, obtained from the temperature dependence of binding constants (Table 3), were analyzed through the Van't Hoff plot depicted in Figure 5 ( $\ln K_{sv}$  versus  $1/T$ ). This analysis demonstrated that  $\Delta G$  is negative at both temperatures examined, indicating that the binding process is spontaneous and thermodynamically favorable. The positive  $\Delta H$  (+5.74 kJ/mol) indicates an endothermic binding process, consistent with the disruption of ordered water molecules at hydrophobic surfaces. Additionally, the positive  $\Delta S$  (+99.8 J/mol·K) suggests an increase in system entropy, consistent with hydrophobic-driven binding and

release of structured water molecules upon complex formation (Table 4).

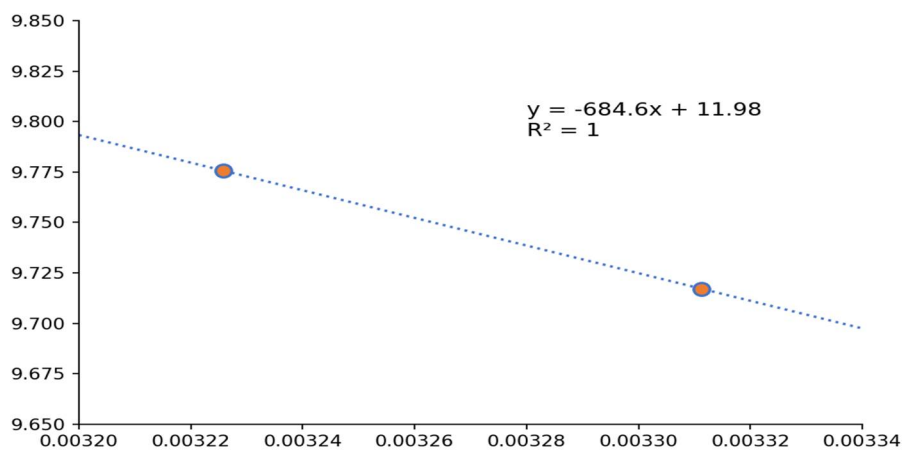
**Table 3. Temperature dependence of binding constants**

Temperature (K)	$K_{sv}$ ( $\mu\text{M}^{-1}$ )	$\ln K_{sv}$	$1/T$ ( $\text{K}^{-1}$ )
302	0.0166	+9.717	0.00331
310	0.0176	+9.776	0.00323

\*  $K_{sv}$  values were converted to  $\text{M}^{-1}$  ( $1.66 \times 10^4$  and  $1.76 \times 10^4 \text{M}^{-1}$ ) before logarithmic transformation for Van't Hoff analysis.

**Table 4. Thermodynamic parameters for Molnupiravir-BSA binding**

Parameter	Value	Unit
$\Delta H$	+5.74	kJ/mol
$\Delta S$	+99.8	J/mol·K
$\Delta G_{302}$	-24.4	kJ/mol
$\Delta G_{310}$	-25.2	kJ/mol

Figure 5. Van't Hoff plot ( $\ln K_{sv}$  vs  $1/T$ ) for Molnupiravir-BSA interaction.

**Binding constants and stoichiometry.** Table 5 and Figure 6 illustrate that the binding constant increased from  $0.032 \mu\text{M}^{-1}$  at 302K to  $0.038 \mu\text{M}^{-1}$  at 310K. This indicates that binding affinity was stronger at physiological temperature. The number of binding sites ( $n$ ) was approximately 0.84 at 302K and

0.83 at 310K, suggesting that Molnupiravir and BSA interact in a 1:1 molar ratio. The consistent  $n$  values at both temperatures substantiate the binding hypothesis and imply that each BSA molecule accommodates roughly one Molnupiravir molecule.

**Table 5. Data for binding constant determination.**

Temperature (K)	Binding Constant $K$ ( $\mu\text{M}^{-1}$ )	Number of Binding Sites (n)	$R^2$
302	0.032	0.84	0.992
310	0.038	0.83	0.994

**Molecular docking analysis.** Molecular docking demonstrated that molnupiravir binds specifically to

Sudlow site I on BSA, with a binding affinity of  $-7.9$  kcal/mol, consistent with the outcomes of fluorescence spectroscopy. It occupies a hydrophobic cavity, stabilized through hydrogen bonds with GLY327 and ARG208, carbon-hydrogen bonds with ALA212 and LYS350 and interactions with LYS211, VAL215, ALA349, and LEU346. This suggests a single primary binding site and a 1:1 binding ratio.

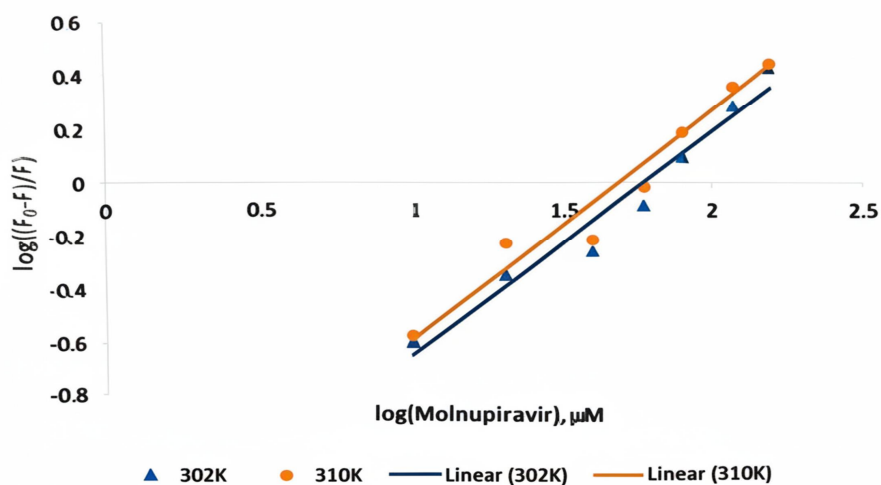


Figure 6. Double logarithmic plots for determining binding constants and binding sites at 302K and 310K

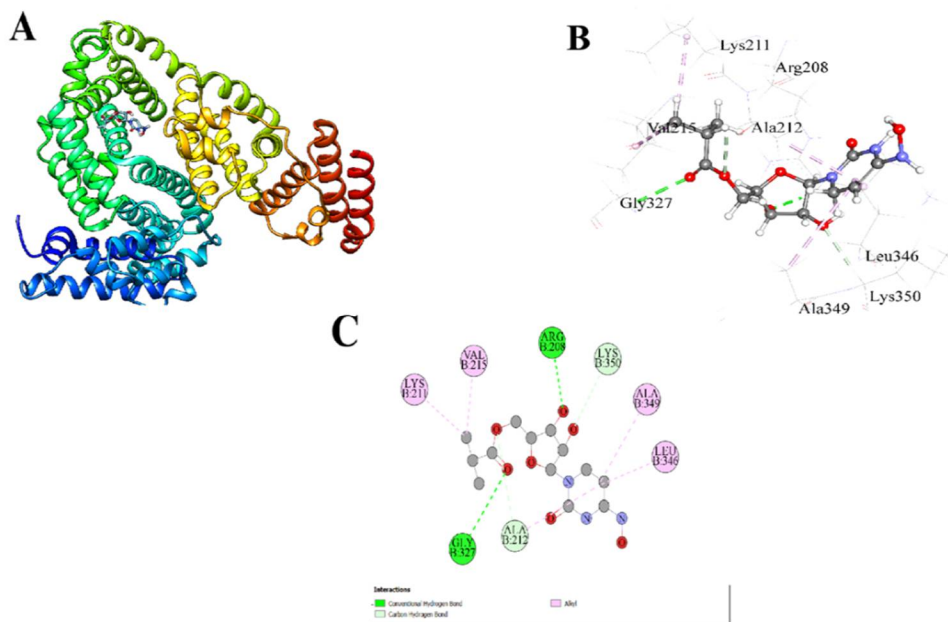


Figure 7. (A & B) Three-dimensional representation of the interaction between molnupiravir and BSA, (C) Two-dimensional representation of the interaction between molnupiravir and BSA.

This study evaluates how Molnupiravir interacts with bovine serum albumin (BSA) via fluorescence spectroscopy and molecular docking, offering insight into its protein-binding behavior under physiological conditions. It analyzes quenching mechanisms, binding parameters and thermodynamics, aiding understanding of its pharmacokinetics. Fluorescence quenching at 280 and 293 nm shows perturbation of BSA's tryptophan residues (Trp134 and Trp212). This implication is inferred from molecular docking results rather than from direct experimental identification of the individual residue. Stronger quenching at 293 nm indicates these residues are key in binding.<sup>1,4,15</sup> Docking locates Molnupiravir at Sudlow site I, near Trp212, implying fluorescence changes result from microenvironmental and conformational shifts near this site, not direct contact.<sup>1,4,17,18,20</sup>

The Stern–Volmer analysis indicated that quenching constants increased with temperature, demonstrating a dynamic quenching mechanism. Elevated temperatures enhance diffusion and collision frequency, thereby boosting quenching efficiency and suggesting rapid binding–dissociation between Molnupiravir and BSA rather than stable complexes. Thermodynamic data showed negative Gibbs free energy values at both temperatures, confirming spontaneous binding with moderate affinity. Positive enthalpy and entropy changes suggest an interaction driven mainly by hydrophobic forces, stabilized by hydrophobic interactions, with hydrogen bonds involving GLY327 and ARG208 providing additional stability.

Docking results indicate hydrogen bonds between GLY327 and ARG208, along with van der Waals and hydrophobic contacts within the Sudlow site I cavity. The interaction with ARG208 is a charge-assisted hydrogen bond that supports stability without significantly affecting thermodynamics.<sup>16,19</sup> Spectroscopic and computational data show hydrophobic interactions predominantly drive Molnupiravir–BSA binding, consistent with the positive  $\Delta H$  and  $\Delta S$  observed, while hydrogen bonds involving GLY327 and ARG208 offer additional

stabilization.<sup>19</sup> The hydrophobic driving forces are validated by docking results, which highlight extensive alkyl and hydrophobic contacts with LYS211, VAL215, ALA349 and LEU346 at Sudlow site I. Binding constants suggest a moderate affinity that slightly increases with temperature. This trend aligns with the entropy-driven interaction: as temperature rises, the favorable T $\Delta S$  contribution outweighs the endothermic  $\Delta H$ , resulting in a more negative  $\Delta G$  at 310 K (–25.2 kJ/mol) compared to 302 K (–24.4 kJ/mol). The  $n$  values of approximately 0.84 at 302 K and 0.83 at 310 K are close to unity, which, in previously published drug–BSA fluorescence quenching studies, is conventionally interpreted as indicating approximately one primary binding site per protein molecule.<sup>21</sup> This interpretation is further corroborated by the molecular docking result, which localizes molnupiravir to a single site at Sudlow site I. Temperature influences binding strength but not stoichiometry, indicating a stable interaction.<sup>17,18</sup>

Molnupiravir's moderate binding affinity means most remains unbound, enabling effective antiviral activity and some transport. Rapid equilibria allow dose flexibility. Compared to highly protein-bound antivirals, it has weaker, more dynamic albumin binding, reducing displacement risk, though studies are needed. These traits suggest favorable pharmacokinetics and clarify its *in vivo* behavior.

Overall, this study provides an original *in vitro* characterization of molnupiravir–BSA binding, establishing a foundational pharmacological profile for the parent prodrug. Nevertheless, *in vitro* characterization of the parent prodrug's albumin-binding properties remains justified. Because molnupiravir contacts plasma proteins during pre-systemic absorption before enzymatic conversion, potentially affecting early distribution kinetics.<sup>9,11</sup> On top of that, to our knowledge, no prior study had characterized the BSA-binding properties of molnupiravir using fluorescence quenching spectroscopy and molecular docking, making the present findings an original mechanistic contribution to its pharmacological characterization.

### Methodological Considerations and Limitations

However, some limitations should be considered. BSA was used as a model protein for HSA, which shares 76% homology but may differ in binding-site structure, particularly at the Sudlow site I, affecting binding parameters; direct studies with HSA are more relevant for therapy. Experiments used simple buffer systems without other plasma components influencing protein binding. The study focused solely on Molnupiravir, not its main metabolite, N4-hydroxycytidine, which may bind differently. Fluorescence quenching provides clues about nearby tryptophan residues, but other methods like circular dichroism or isothermal titration calorimetry reveal more about structure and thermodynamics. Although the two-temperature-point approach is widely used in drug-BSA fluorescence quenching studies and gives high linearity ( $R^2 > 0.99$ ), future studies should include three or more temperature points to improve the robustness of the Van't Hoff regression and better estimate  $\Delta H$  and  $\Delta S$  values.

### Clinical Significance and Future Directions

This study's findings inform the clinical application of Molnupiravir for COVID-19. Its moderate protein binding suggests dose adjustments are unnecessary in hypoalbuminemic patients, as free drug levels are likely to remain within therapeutic ranges. The modest binding and dynamic interactions indicate a low risk of displacement interactions with drugs such as dexamethasone or anticoagulants. An increased binding affinity at 310 K ( $\Delta G = -25.2$  kJ/mol vs.  $-24.4$  kJ/mol at 302 K) implies febrile conditions cause only minor changes in protein binding. Thermodynamic data reveal that hydrophobic interactions mainly drive binding, supported by hydrogen bonds that enhance stability and reduce competition with drugs primarily relying on electrostatic mechanisms. Further studies are required, including with HSA, active metabolite N4-hydroxycytidine, co-administered drugs, disease states and clinical data.

### CONCLUSION

This study examined Molnupiravir's interaction with bovine serum albumin (BSA), finding moderate binding with constants of  $0.032 \mu\text{M}^{-1}$  at 302 K and  $0.038 \mu\text{M}^{-1}$  at 310 K. Fluorescence quenching indicated a dynamic mechanism, with Stern-Volmer constants rising from  $0.0166 \mu\text{M}^{-1}$  at 302 K to  $0.0176 \mu\text{M}^{-1}$  at 310 K, suggesting collisional quenching rather than stable complex formation. Thermodynamic data indicate a spontaneous process primarily driven by hydrophobic interactions, with positive  $\Delta H$  and  $\Delta S$  values. Negative Gibbs free energy values confirm spontaneous binding at physiological temperatures. Molecular docking shows the drug binds at Sudlow site I (subdomain IIA) of BSA, forming hydrogen bonds with GLY327 and ARG208, along with hydrophobic interactions, consistent with a 1:1 binding ratio. Fluorescence shifts at 280 and 293 nm suggest binding affects tryptophan environments, particularly in domain II. Overall, Molnupiravir exhibits protein binding, supporting favorable pharmacokinetics for COVID-19 and informing future serum albumin studies.

### ACKNOWLEDGMENT

All authors acknowledged the lab facilities of the Department of Pharmacy, International Islamic University Chittagong.

### CONFLICT OF INTEREST

No conflict of interest

### FINANCIAL SUPPORT

The authors did not receive any special grant or support from any organization.

### REFERENCES

1. He, X. M. and Carter, D. C. 1992. Atomic structure and chemistry of human serum albumin. *Nature*. **358**, 209-215.
2. Hage, D. S., Jackson, A., Sobansky, M. R., Schiel, J. E., Yoo, M. J. and Joseph, K. S. 2009. Characterization of drug-protein interactions in blood using high-performance affinity chromatography. *J. Sep. Sci.* **32**, 835-853.

3. McLachlan, A. D. and Walker, J. E. 1977. Evolution of serum albumin. *J. Mol. Biol.* **112**, 543–558.
4. Sugio, S., Kashima, A., Mochizuki, S., Noda, M. and Kobayashi, K. 1999. Crystal structure of human serum albumin at 2.5 Å resolution. *Protein Eng.* **12**, 439–446.
5. Bernal, A. J., Gomes Da Silva, M. M., Musungaie, D. B. et al. 2022. Molnupiravir for oral treatment of Covid-19 in nonhospitalized patients. *N. Engl. J. Med.* **386**, 509–520.
6. Rahman, T., Islam, M. S., Paul, S. et al. 2023. Prescription patterns in an intensive unit of COVID-19 patients in Bangladesh: A cross-sectional study. *Health Sci. Rep.* **6**, e1711.
7. Sheahan, T. P., Sims, A. C., Zhou, S. et al. 2020. An orally bioavailable broad-spectrum antiviral inhibits SARS-CoV-2 in human airway epithelial cell cultures and multiple coronaviruses in mice. *Sci. Transl. Med.* **12**, eabb5883.
8. Malone, B. and Campbell, E. A. 2021. Molnupiravir: coding for catastrophe. *Nat. Struct. Mol. Biol.* **28**, 706–708.
9. Maas, B. M., Strizki, J., Miller, R. R. et al. 2024. Molnupiravir: mechanism of action, clinical, and translational science. *Clin. Transl. Sci.* **17**, e13732.
10. Dömötör, O. and Enyedy, É. A. 2023. Evaluation of in vitro distribution and plasma protein binding of selected antiviral drugs (favipiravir, molnupiravir and imatinib) against SARS-CoV-2. *Int. J. Mol. Sci.* **24**, 2849.
11. Painter, W. P., Holman, W., Bush, J. A. et al. 2021. Human safety, tolerability, and pharmacokinetics of molnupiravir, a novel broad-spectrum oral antiviral agent with activity against SARS-CoV-2. *Antimicrob. Agents Chemother.* **65**, e02428-20.
12. Perrin, D. D. **2012**. Buffers for pH and metal ion control. *Springer*.
13. Sharaf, Y. A., El Deeb, S., Ibrahim, A. E., Al-Harrasi, A. and Sayed, R. A. 2022. Two green micellar HPLC and mathematically assisted UV spectroscopic methods for the simultaneous determination of molnupiravir and favipiravir as a novel combined COVID-19 antiviral regimen. *Molecules.* **27**, 2330.
14. Jain, P., Bhamare, M. and Surana, S. 2022. Quantitative estimation of molnupiravir by UV-spectrophotometric method. *Int. J. Pharm. Chem. Anal.* **9**, 35-39.
15. Lakowicz, J. R. 2006. Instrumentation for fluorescence spectroscopy. In: Principles of Fluorescence Spectroscopy. *Springer*, 27-61.
16. Koly, S. F., Kundu, S. P., Kabir, S., Amran, M. S. and Sultan, M. Z. 2015. Analysis of aceclofenac and bovine serum albumin interaction using fluorescence quenching method for predictive, preventive, and personalized medicine. *EPMA J.* **6**, 24.
17. Papadopoulou, A., Green, R. J. and Frazier, R. A. 2005. Interaction of flavonoids with bovine serum albumin: a fluorescence quenching study. *J. Agric. Food Chem.* **53**, 158–163.
18. Sun, S. F., Zhou, B., Hou, H. N., Liu, Y. and Xiang, G. Y. 2006. Studies on the interaction between oxaprozin-E and bovine serum albumin by spectroscopic methods. *Int. J. Biol. Macromol.* **39**, 197-200.
19. Ross, P. D. and Subramanian, S. 1981. Thermodynamics of protein association reactions: forces contributing to stability. *Biochemistry.* **20**, 3096-3102.
20. Goncharenko, N. A., Dmytrenko, O. P., Kulish, M. P. et al. 2020. Mechanisms of the interaction of bovine serum albumin with anticancer drug gemcitabine. *Mol. Cryst. Liq. Cryst.* **701**, 59–71.
21. Katrahalli, U., Kalanur, S. S. and Seetharamappa, J. 2010. Interaction of bioactive Coomassie Brilliant Blue G with protein: insights from spectroscopic methods. *Sci. Pharm.* **78**, 869–880.